Chemosphere 336 (2023) 139119

Contents lists available at ScienceDirect

Chemosphere

journal homepage: www.elsevier.com/locate/chemosphere

Source-oriented ecological and resistome risks associated with geochemical enrichment of heavy metals in river sediments

Zhimin Yang [a], Chunhui Li [a], Haiyang Chen [b,*], Xin Shan [b], Jinping Chen [b], Jianhang Zhang [c], Shaoda Liu [d,**], Qiang Liu [a], Xuan Wang [d]

[a] Key Laboratory for Water and Sediment Sciences of Ministry of Education, School of Environment, Beijing Normal University, Beijing, 100875, China
[b] Engineering Research Center of Ministry of Education on Groundwater Pollution Control and Remediation, College of Water Sciences, Beijing Normal University, Beijing, 100875, China
[c] Faculty of Geographical Science, Beijing Normal University, Beijing, 100875, China
[d] State Key Laboratory of Water Environment Simulation, School of Environment, Beijing Normal University, Beijing, 100875, China

HIGHLIGHTS

- A multidisciplinary-based framework has been proposed for analyzing HM risks.
- Apportionment results of PMF and Unmix models were similar and complementary.
- Industrial and agricultural sources were the main contributors of HM ecological risks.
- Diverse ARGs were identified and correlated with the geochemical enrichment of HMs.
- This work facilitates the progress of characterizing source-oriented risks of HMs.

GRAPHICAL ABSTRACT

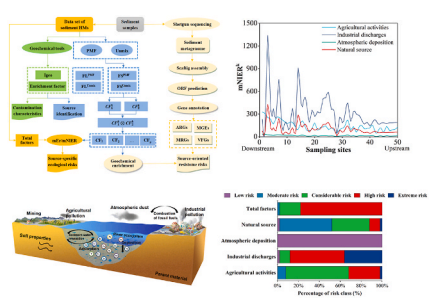

ARTICLE INFO

Handling Editor: Lena Q. Ma

Keywords:
Heavy metals
Source apportionment
Source-specific ecological risk
Environmental forensic models
Antibiotic resistome risk
River sediments

ABSTRACT

Heavy metals (HMs) pose ecological and resistome risks to aquatic systems. To efficiently develop targeted risk mitigation strategies, apportioning HM sources and assessing their source-oriented risks are essential. Although many studies have reported risk assessment and source apportionment of HMs, yet few have explored source-specific ecological and resistome risks associated with geochemical enrichment of HMs in aquatic environments. Therefore, this study proposes an integrated technological framework to characterize source-oriented ecological and resistome risks in the sediments of a plain river in China. Several geochemical tools quantitatively showed Cd and Hg had the highest pollution levels in the environment, with 19.7 and 7.5 times higher than their background values, respectively. Positive matrix factorization (PMF) and Unmix were comparatively used to apportion sources of HMs. Essentially, the two models were complementary and identified similar sources including industrial discharges, agricultural activities, atmospheric deposition and natural background, with contributions of 32.3–37.0%, 8.0–9.0%, 12.1–15.9% and 42.8–43.0%, respectively. To analyze source-specific ecological risks, the apportionment results were integratively incorporated into a modified ecological risk index. The results showed anthropogenic sources were the most significant contributors to the ecological

* Corresponding author.
** Corresponding author.
E-mail addresses: chen.haiyang@bnu.edu.cn (H. Chen), liushaoda@bnu.edu.cn (S. Liu).

https://doi.org/10.1016/j.chemosphere.2023.139119
Received 28 April 2023; Received in revised form 27 May 2023; Accepted 1 June 2023
Available online 9 June 2023
0045-6535/© 2023 Elsevier Ltd. All rights reserved.

risks. Particularly, industrial discharges majorly contributed high- (44%) and extremely high (52%) ecological risk for Cd, while agricultural activities posed a greater percentage of considerable-(36%) and high- (46%) ecological risk for Hg. Furthermore, the high-throughput sequencing metagenomic analysis identified abundant and diverse antibiotic resistance genes (ARGs), including some carbapenem-resistance genes and emerging genes such as *mcr*-type in the river sediments. Network and statistical analyses displayed significant correlations between ARGs and geochemical enrichment of HMs ($\rho > 0.8$; P-value <0.01), indicating their important impacts on resistome risks in the environment. This study provides useful insights into risk prevention and pollution control of HMs, and the framework can be made applicable to other rivers facing environmental challenges worldwide.

1. Introduction

Heavy metal pollution is one of the most serious environmental issues, which may have far-reaching impacts on ecosystems and human health owing to its toxicity, persistence and potential bioaccumulation/biomagnification (Gu et al., 2021; Zhang et al., 2021; Yan et al., 2022). Rivers often face the contamination of heavy metals (HMs) originating from intensive agriculture, increasing industrialization, and rapid urbanization (Xia et al., 2020). In particular, HMs can accumulate in river sediments via deposition, adsorption, and coagulation (Chen et al., 2021a). When the river conditions change, HMs in sediments will be released to the water again resulting in secondary pollution. The pollution of HMs in rivers can not only negatively affect farming, irrigation and normal crop growth, but also pose a potential threat to aquatic ecosystems and human health, such as via the food chain (Hakanson, 1980; Chen et al., 2019a). Also, researchers have demonstrated that HMs could co-select antimicrobial resistance (AMR), causing the prevalence and spread of antibiotic resistance genes (ARGs) in river ecosystems (Baker-Austin et al., 2006; Li et al., 2021); and AMR has been a major global public health concern (UNEP, 2017).

Understanding the characteristics and sources of heavy metal risk is imperative to prevent and control the environmental pollution (Proshad et al., 2022). Over the past years, many methods have been developed and applied for risk assessment of HMs in various environmental media, such as contamination factor (Huang et al., 2022a), enrichment factor (Magesh et al., 2021), geoaccumulation index (Yan et al., 2022), potential ecological risk index (Huang et al., 2022b), Nemerow integrated pollution index (Men et al., 2020), sediment quality guidelines (Proshad et al., 2022) and so on. Likewise, abundant methods have been conducted for source apportionment studies, such as correlation analysis (Xia et al., 2020), principal component analysis (PCA) (Proshad et al., 2022), absolute principal component scoremultiple linear regression (APCS-MLR) (Yan et al., 2022), positive matrix factorization (PMF) (Huang et al., 2022a), multilinear engine-2 (Men et al., 2021), chemical mass balance (Wang et al., 2015), Unmix model (Xu et al., 2014), isotope tracer technique (Huang et al., 2015), referential source fingerprints (Li et al., 2020), geographical detector method (Fan et al., 2020) and so on. However, although many research have evaluated the ecological risk of HMs and apportioned their sources in river sediments, the source-specific ecological risks have not received sufficient attention (Li et al., 2021). Notably, the contributions of apportioned sources are not in accordance with the results of source-oriented risk assessment (Fei et al., 2022; Yan et al., 2022). Accordingly, quantitative source-specific risk apportionment is essential since the source-oriented risk analysis is more effective for designing targeted risk mitigation and source control strategies (Shi et al., 2019; Men et al., 2020; Xia et al., 2021). However, accurately apportioning the source-specific risks of sedimental HMs is still a challenging work due to the high spatial heterogeneity induced by anthropogenic and natural sources in the environment (Xia et al., 2020; Guo et al., 2021).

Aside from that, the prevalence of ARGs in the river ecosystem is an increasing concern, and HMs are considered as one of the significant co-selection forces in the evolution and spread of ARGs (Chen et al., 2019b; Zhang et al., 2020; Liu et al., 2022). Previously, several investigations found the association of ARGs with HMs in river system; however, few explored the influence of source-oriented geochemical enrichment of HMs on ARGs in river sediments (Zhang et al., 2022a). ARGs can be developed and dispersed through the geochemical accumulation of HMs such as via co-resistance (Xu et al., 2017), cross-resistance (Wang et al., 2021), and/or co-regulation mechanisms (Baker-Austin et al., 2006). More interestingly, recent studies showed the geochemical index (i.e., enrichment factor) was favorable for exploring the influence of HMs on microbial communities and ARGs. This is because geochemical enrichment factors hold more information to reveal the impact of human activities, such as overall contamination status and pollution sources (Li et al., 2021; Zhang et al., 2022a).

To address these issues, an integrated multidisciplinary-based technological framework was developed and applied for characterizing the source-oriented ecological and resistome risks associated with the geochemical enrichment of HMs in the sediments of a plain river in China, by integrating forensic models (positive matrix factorization, and Unmix) and metagenomic analysis. The two forensic models were recommended by the U.S. Environmental Protection Agency (U.S. EPA) for source apportionment (Keeler et al., 2006). Relatively, Unmix is scarcely applied for source apportionment of HMs in river sediments, and the issue of whether they can be used together and what differences there are in their results remains to be explored. Herein, the two models were jointly applied to quantitatively identify the possible sources of HMs, and their apportionment results were integratively incorporated into a modified index to evaluate the source-specific ecological risks of sediment HMs. Similarly, the apportionment results were also used to explore the influence of source-oriented geochemical enrichment of HMs on antibiotic resistome, and the high-throughput sequencing-based metagenomic analysis was employed to characterize the prevalence of antimicrobial resistance. Fig. 1 illustrates the proposed framework schematically. The findings can provide an important basis to address the environmental risk challenge of HMs, and the methodology solution will offer a new insight for a better understanding of HM risks in other water environments worldwide.

2. Materials and methods

2.1. Study area

The study area (Nanxi River) is situated in Yixing city of Jiangsu Province, Eastern China (31°07′ N~31°37′ N, 119°31′ E~120°03′ E) (Fig. 2a). It is one of the main tributaries of Lake Tai which is the third largest freshwater lake in China. However, multiple human-mediated stressors threaten the area due to the sluggish flow and high intensity of human development in the plain river networks, making it one of the most seriously polluted ecosystems worldwide (Ouyang et al., 2016). In the area, the annual average precipitation and temperature are 1229.9 mm and 16.5 °C, respectively; and over 60% of rainfall is concentrated during shorter periods between May and September. The proportion of cropland is the largest (50.5%), followed by the impervious surface (18.0%) (Fig. 2b).

2.2. Sample collection, chemical analysis and shotgun metagenomic sequencing

The river sediments were collected from 50 sampling sites along the Nanxi River, as shown in Fig. 2c. At each site, a stainless-steel grab sampler was used to collect samples from the topmost 5 cm of the riverbed with three replications. Then, the three sub-samples were mixed thoroughly into two composite samples. One was used for metal analysis, and kept in the amber polyethylene plastic bottle (50 mL). The other was used for DNA extraction, and placed in the sterile polypropylene centrifuge tube (10 mL). After collection, all samples were kept in the refrigerator at 4 °C and then transported to lab on dry ice immediately.

The chemical analyses of samples were conducted at the Analysis and Testing Center of Beijing Normal University. Twelve metals (Cr, chromium; Cd, cadmium; As, arsenic; Hg, mercury; Pb, lead; Cu, copper; Zn, zinc; Ni, nickel; Mn, manganese; V, vanadium; Be, beryllium; Co, cobalt) were determinated for each sample. To ensure the analysis quality, several necessary control measures of laboratory were adopted, including reagent blank analysis, spiked sample recovery, and standard calibration. Details on the chemical analysis and quality control can be found in Text S1.

To characterize the ARG risk levels in river sediments, twenty-one samples were selected for metagenomic sequencing. For each sediment sample, the total DNA was extracted using the TIANamp DNA Kit for Soil as instructed by the manufacturer. The high-quality DNA was employed to construct library. Metagenomic shotgun sequencing was performed on the Illumina HiSeq platform with 150 bp paired-end strategy (Li et al., 2021).

2.3. Geochemical tools for contamination assessment

Several geochemical indexes were applied to identify the metal contamination characteristics in the river sediments, including the enrichment factor (*EF*) and geoaccumulation index (I_{geo}). Among them, the *EF* is used to characterize the contamination enrichment level of elements, while the I_{geo} is a geochemical approach for assessing the contamination status of metals according to their background values (Magesh et al., 2021). Herein, aluminum as the third largest component of Earth's crust was selected as a reference metal for *EF* calculations (Li et al., 2021), since it was uniformly distributed spatially with the lowest coefficient of variation (14.9%) among the studied metals. Details of these indexes can be found in Text S2. Additionally, the Nemerow integrated pollution index (*NIPI*) was used to explain the overall pollution status of metals. It is calculated as follows (Yan et al., 2022):

$$NIPI = \sqrt{\frac{CF_{\text{ave}}^2 + CF_{\text{max}}^2}{2}} \quad (1)$$

where CF_{ave} and CF_{max} represent the average and maximum contamination factors of the corresponding metals, respectively.

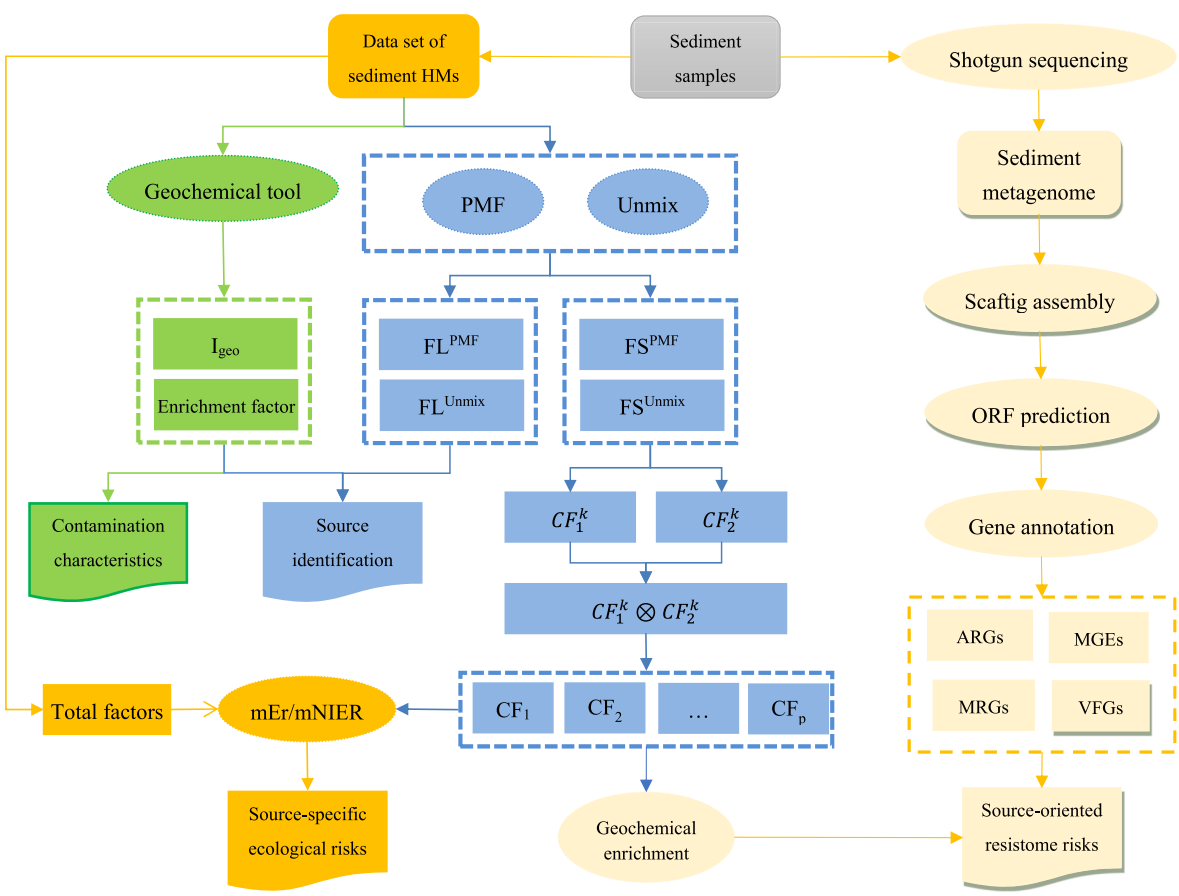

Fig. 1. Schematic diagram of the technological framework for characterizing source-oriented ecological and resistome risks. HMs: heavy metals; PMF: positive matrix factorization; I_{geo}: geo-accumulation index; FL^{PMF} and FL^{Unmix} represent the factor loadings derived by PMF and Unmix, respectively; FS^{PMF} and FS^{Unmix} represent the factor scores derived by PMF and Unmix, respectively; CF_1^k and CF_2^k represent the concentration fraction contributed by the *k*th source (k = 1,2, …p, p is the number of sources) from PMF and Unmix, respectively; ⊗ is the composition operator; $CF_{1,2,\ldots p}$: concentration fraction for the *k*th source (k = 1,2, …p); mEr: modified ecological risk index; mNIER: modified Nemerow integrated ecological risk index; ORF: open reading frames; ARGs: antibiotic resistance genes; MRGs: metal resistance genes; MGEs: mobile genetic elements; VFGs: virulence factor genes.

2.4. Environmental forensic models

2.4.1. PMF

PMF is an advance receptor model, which is free of non-negative constraints thus generating an explainable physical mechanism for the factor scores (Proshad et al., 2022). The model has been developed iteratively for source apportionment studies (U.S. EPA, 2014). In general, a date set including the concentrations of pollutants and their associated uncertainty results are used as inputs for model calculations. The original datasets are decomposed into factor contributions and loadings by minimizing the objective function for identifying pollution sources and their impact intensities (Men et al., 2020; Xia et al., 2020). Multilinear engine (ME-2) was adopted for solving the PMF problem in the study. Details on its principle can be found in Text S3.

2.4.2. Unmix

Unmix is another receptor model recommended by the U.S. EPA. The model uses the self-modeling curve resolution technique and produces source apportionment results automatically based on the selected components (Keeler et al., 2006). The Unmix algorithm finds edges in N-dimensional spaces from sets of points, and the sources can be identified by the edges of projected data (Xu et al., 2014). Compared to the PMF model, Unmix does not require the input of information on the number of sources and the uncertainty of concentration data, which reduces the influence of subjective factors (U.S. EPA, 2007). More details on Unmix can be found in Text S3.

2.5. Source-oriented ecological risk assessment

2.5.1. The modified ecological risk index

A modified method was used to characterize the ecological risks of HMs in this study. The formulas are as follows:

$$mRI = \sum_{i=1}^{n} mE_r^i \tag{2}$$

$$mE_r^i = T_r^i \times EF_i = T_r^i \times \frac{C_i/B_i}{C_r/B_r} \tag{3}$$

where mE_r^i, T_r^i and EF_i are the modified ecological risk, toxic response factor, and enrichment factor for the ith metal, respectively; n is the number of metals considered; C_i and B_i refer to the measured value and background value for the ith metal, respectively; C_r and B_r represent the measured and background values of reference normalization metal. Compared to the conventional potential risk index (RI) proposed by Hakanson (1980), the mRI not only focuses on the pollution concentrations, synergistic effects of multiple elements, and toxicity and sensitivity of pollutants, but also considers their different toxic response factors, thus resulting in a more accurate evaluation (Men et al., 2020; Li et al., 2021).

2.5.2. Source-specific ecological risk assessment

The source-specific ecological risk of sediment HMs was analyzed by effectively combining the source contribution results and risk assessment. First, the contribution concentration of metals from each identified source was determined jointly by the apportionment results of PMF and Unmix models in the following way:

$$\begin{cases} CF_{ij}^{k1} = f_{ij}^{k1} \times C_{ij} \\ \sum_{k1=1}^{p} f_{ij}^{k1} = 1 \end{cases} \tag{4}$$

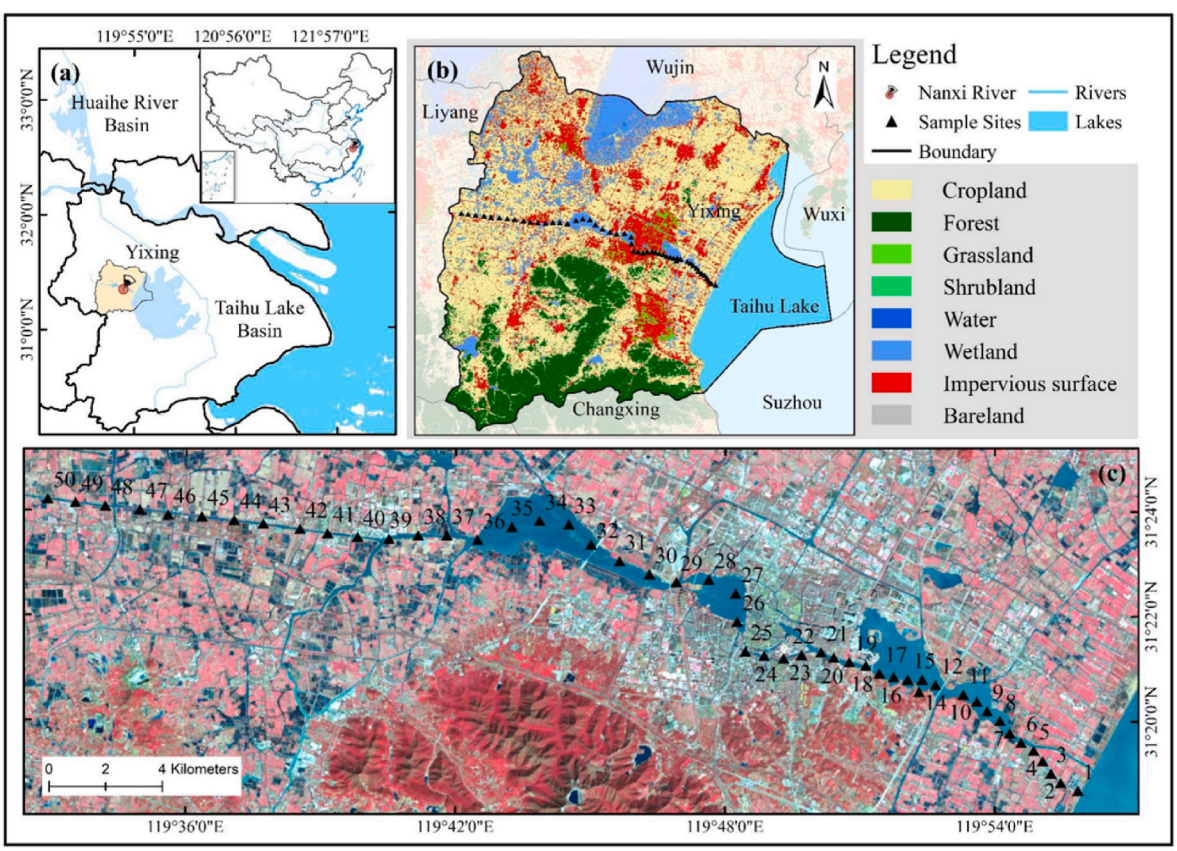

Fig. 2. Maps of the study area: (a) location; (b) land use types; (c) sampling sites.

$$\begin{cases} CF_{ij}^{k2} = f_{ij}^{k2} \times C_{ij} \\ \sum_{k2=1}^{p} f_{ij}^{k2} = 1 \end{cases} \quad (5)$$

$$CF_{ij}^{k} = CF_{ij}^{k1} \otimes CF_{ij}^{k2} \quad (6)$$

where CF_{ij}^{k1} and CF_{ij}^{k2} represent the concentration fraction of ith metal in jth sample contributed by kth source from PMF and Unmix model, respectively; f_{ij}^{k1} and f_{ij}^{k2} represent the corresponding contribution fraction of kth source to ith metal in jth sample from PMF and Unmix, respectively; C_{ij} represents the measured contents of ith metal in jth sample; p represents the number of sources; CF_{ij}^{k} represents the joint concentration fraction from PMF and Unmix (k = 1,2, …p); $\otimes$ refers to the composition operator. In the study, arithmetical average was used as the composition operator.

Then, the contributions of each identified source for HMs from each sampling site were imported into the modified ecological risk model, as follows:

$$mEr_i^k = Tr_i \times EF_i^k = Tr_i \times \frac{C_i^k / B_i}{C_r^k / B_r} \quad (7)$$

where mEr_i^k, EF_i^k and C_i^k are the modified ecological risk index, enrichment factor, and contribution content for ith metal from kth source, respectively; C_r^k is reference element content from kth source.

In addition, to eliminate the accumulation risk associated with metal numbers, the modified integrated ecological risk was also calculated for each identified source, as follows:

$$mNIER^k = \sqrt[2]{\frac{\left(mEr_{Avg}^k\right)^2 + \left(mEr_{Max}^k\right)^2}{2}} \quad (8)$$

where $mNIER^k$ represents the modified Nemerow integrated ecological risk index of kth source; mEr_{Avg}^k and mEr_{Max}^k refer to the average and maximum values of the modified ecological risk model from kth source of all metals, respectively. Table S1 shows the relationships between the indexes and ecological risk levels.

2.6. Antibiotic resistome risk identification

2.6.1. Metagenomic assembly and open reading frame prediction

The description of metagenomic assembly and gene prediction was detailed in our previous study (Chen et al., 2019b). In short, the raw data was first filtered to eliminate the low-quality reads, and MEGAHIT (v1.1.2) was used to assemble the quality-filtered reads. Then, the scaftigs were used to identify open reading frames (ORFs) by utilizing MetaProdigal (v2.6.3), and the ORFs were gathered to construct a non-redundant gene catalog by applying CD-HIT (v4.6.8) (Zhang et al., 2022b).

2.6.2. Annotation of ARGs, metal resistance genes and microbiome

The ARGs and metal resistance genes (MRGs) were annotated by searching the predicted ORFs against the DeepARG database and the BacMet database using Diamond (v2.0.9), respectively (Chen et al., 2021b). For taxonomy annotation, the ORFs were aligned to the proGenomes database using Kaiju (v1.6.3) with a Burrows-Wheeler transform (Zhang et al., 2022a).

2.6.3. Antibiotic resistome risk identification

The ARGs presenting on the mobile genetic elements (MGEs) hosted by human bacterial pathogens have a high resistome dissemination risk (Martínez et al., 2015). To annotate MGEs and virulence factors (VFs), the metagenomic sequences were aligned against the MGE and VF databases, respectively, similarly to the analysis of ARGs annotations (Zhang et al., 2022a). Afterwards, the co-occurrence of MGEs and VFs with ARGs was investigated to evaluate the possible environmental risks of ARGs dissemination. Furthermore, we analyzed the associations between ARGs and source-oriented enrichment factors of sediment HMs to explore the source-specific effects of geochemical behaviors on antibiotic resistome risks.

3. Results and discussion

3.1. Overall contamination risk characteristics of HMs in the river sediments

In the study, we measured twelve HMs in the river sediments and analyzed their contamination characteristics using several geochemical indexes. The average concentration and ranges for Cr, Cd, As, Hg, Pb, Cu, Zn, Ni, Mn, V, Be, and Co were shown in Table 1, as well as other descriptive statistics. Relatively, the contents for most of the HMs in the Nanxi River were lower than those in other regions around the world (Table S2). Nevertheless, the river sediments were seriously polluted by some HMs when compared to the local background values, such as Cd, Hg, Zn, and Cu (Table 1). Specifically, the average concentrations of Cd and Hg were about 19.7 and 7.5 times higher than their backgrounds, respectively. Also, Zn, Pb, Cu, Ni, Mn, and Cr showed a high exceedance rate with 98%, 96%, 86%, 68%, 66%, and 56%, respectively. The geochemical assessment results further showed that Cd and Hg had high pollution levels in the river sediments; and Zn, Cu, Pb, Mn, Ni, and As lay moderate levels. As a whole, Cd, Hg, Zn, and Cu were recognized as the priority pollutants in the study area. Not strangely, a high level of Cd was also reported in the Yangtze River (Luo et al., 2021), Yellow River (Yan et al., 2016), and Pearl River Delta (Xiao et al., 2022), showing that Cd contamination was a widespread environmental issue in China. As shown in Fig. S1, the *CF* and *EF* indices followed the order of Cd > Hg > Zn > Cu > Pb > Mn > Ni > As. According to the I_{geo}, Cd and Hg were identified as significantly polluted metals, with I_{geo} values of 3.44 and 2.17, respectively. The E_r^i and mE_r^i values of all studied metals except Cd and Hg exhibited low ecological risks (<40). Comparatively speaking, the pollution levels of HMs in the environment followed the order of Cd > Hg > Zn > Cu > Pb (Table S3). Notably, the Nemerow integrated pollution index showed 98% of the sampling sites belonged to the seriously polluted domain.

Spatially, the concentrations of metals in downstream sites (section A) were higher ($p < 0.05$) than those in other regions, and Cd and Hg were mainly found in the area (Fig. S2). Indeed, the coefficients of variation for Cd and Hg were more than 45% (Table 1), indicating their spatial distributions varied among different sites (Magesh et al., 2021; Yan et al., 2022). Previous research showed that anthropogenic factors were strongly associated with the elements with high coefficients of variation (Zhang et al., 2019; Xia et al., 2020). On the contrary, Section *E* was the least polluted area. Specifically, all metals except Hg had the lowest concentrations at the sampling sites near the Longbei Mountain Forest Park, which was the largest urban ecological park in Jiangsu Province of China. Many studies also showed the heavy metal contamination in rivers and lakes in eastern China was generally higher than that in the west (Table S2), which was closely related to the relatively higher level of industrialization and urbanization in plain river network areas (Li et al., 2018; Xia et al., 2021). Notably, Be and Co did not show distinct spatial patterns, indicating they probably originated from natural background.

3.2. Source apportionment of sedimental metals using PMF model

The PMF model was used to reveal the correlation among HMs and quantitatively apportion their sources. The effectiveness of model predictions was determined by the determination coefficients (r^2), and some methods were jointly applied to verify the number of source

Table 1
Descriptive statistics of heavy metals in the river sediments (mg/kg).

	Cr	Cd	As	Hg	Pb	Cu	Zn	Ni	Mn	V	Be	Co
Minimum	8.16	0.20	0.70	0.07	3.89	4.28	32.05	4.33	116	8.66	0.22	1.45
10th	52.44	0.81	5.01	0.11	23.16	22.10	122.40	25.51	553	65.33	1.59	9.69
25th	58.12	0.99	6.18	0.12	27.97	29.45	139.56	29.42	645	70.71	1.70	10.59
50th	77.21	1.26	8.41	0.16	34.03	55.14	194.93	43.60	866	83.11	1.97	13.56
Mean	72.76	1.67	9.62	0.19	36.79	51.94	188.24	40.88	924	80.34	1.88	12.95
Geometric mean	69.38	1.39	8.46	0.17	33.86	45.31	177.71	38.15	854	77.32	1.80	12.33
75th	85.98	1.95	12.36	0.24	45.15	65.38	228.28	49.97	1098	90.20	2.12	14.72
90th	93.31	2.75	16.71	0.32	56.23	81.09	256.61	54.69	1461	97.66	2.23	16.55
Maximum	99.32	7.23	24.62	0.43	67.98	120.79	286.46	66.86	1626	113.70	2.51	18.76
S.D. [a]	17.60	1.20	4.70	0.09	13.70	24.50	55.63	12.64	338	16.08	0.40	3.18
C.V. [b]	0.24	0.72	0.49	0.46	0.37	0.47	0.30	0.31	0.37	0.20	0.21	0.25
Kurtosis	4.77	11.18	4.05	3.24	2.86	3.38	2.80	2.86	2.57	9.24	9.13	4.93
Skewness	−1.02	2.53	1.00	0.91	0.41	0.52	−0.40	−0.48	0.31	−1.67	−2.10	−0.90
T.R.F. [c]	2	30	10	40	5	5	1	5	1	2	1	5
A.B.V. [d]	75.60	0.09	9.40	0.03	22.00	23.40	64.80	32.80	718.00	87.00	2.22	14.60
CSG-grade I [e]	250	0.3	20	0.2	80	150	200	60	- [g]	–	–	–
CSG-grade II [f]	300	0.6	25	0.5	140	200	250	100	–	–	–	–

[a] Standard deviation.
[b] Coefficient of variation (%).
[c] Toxic response factor.
[d] Average background values in local soils.
[e] Chinese soil guideline grade I (GB-15618-1995).
[f] Chinese soil guideline grade II (GB-15618-1995, 6.5 < pH < 7.5).
[g] No data.

factors, including PCA, accumulative percent variance, and Pearson's correlation analysis (Fig. S3). The details can be found in Text S4. The model complexity was established by implementing 100 test runs for each scenario to obtain the minimum value of Q among the several test factors (2–5) (Magesh et al., 2021). Herein, four factors were identified as the optimal means for resolving HM concentration (Fig. 3). With the four–factor solution, almost all metals presented reasonable linear regressions, and the values of r^2 varied from 0.54 (Cd) to 0.99 (Hg). The most meaningful information was retained with a cumulative percent variance of 91.31%. All the residuals of the studied HMs coincided with the normal distribution, and the model performed well with a mean signal-to-noise ratio (S/N) value of 2.14 (>1).

As shown in Fig. 3a, Factor 1 was predominantly represented by Hg and Cu, with contributions of 56.6% and 10.0%, respectively. The average concentrations of Hg and Cu significantly exceeded their background values with obvious enrichment ($EF > 2$), indicating they probably originated from anthropogenic activities. Additionally, they were mainly concentrated on the flat and fertile cropland near Lake Tai with similar spatial distribution patterns (Fig. 2b). Specifically, Cu is a primary element in pesticides and fungicides, which is also related to the application of animal manure (Jiang et al., 2021). Furthermore, Hg and its compounds are commonly used in agricultural fertilizers and

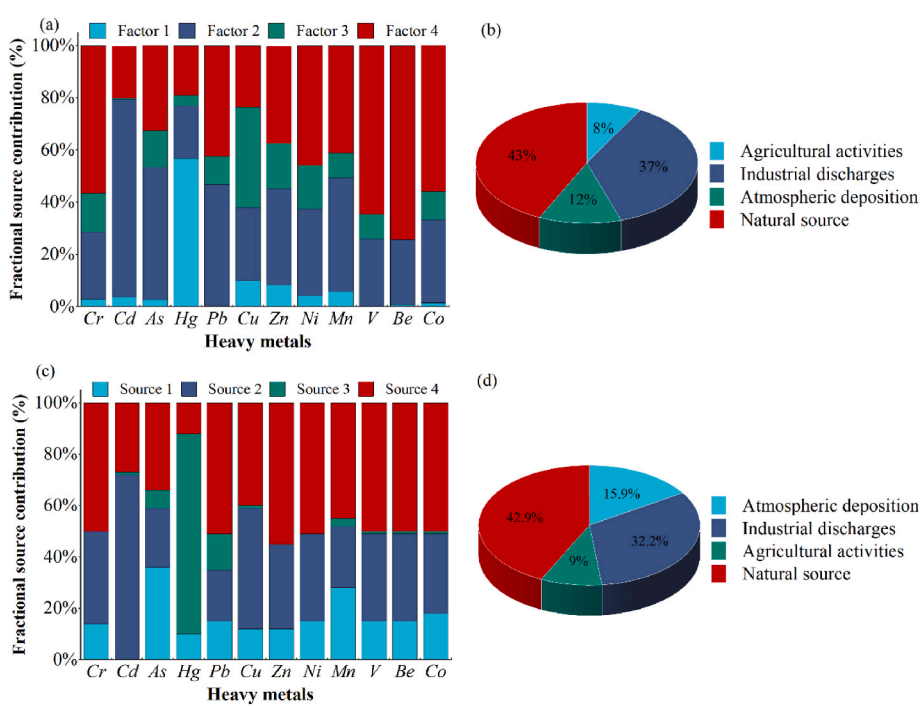

Fig. 3. Factor profiles of heavy metals in the river sediments apportioned by the PMF model (a) and Unmix model (c), and their average contributions from the results of PMF (b) and Unmix (d).

pesticides (Li et al., 2018; Guo et al., 2019; Men et al., 2020). An isotope ratio analysis found that 74–100% of Hg was released into the environment from organic fertilizers used in peri-urban agriculture (Huang et al., 2015). Also, Yan et al. (2022) demonstrated that the aquacultural source was an important contributor to Hg. The Nanxi River was located in the plain river network area, and aquaculture was naturally adapted to the local water environment and climate conditions. Therefore, factor 1 was ascribed to agricultural activities.

Factor 2 had the highest contribution for Cd (75.8%) and moderately loaded on As (50.6%), Pb (46.6%), Mn (43.6%), and Zn (37.0%). Here, the presence of Cd was barely correlated with many metals such as Hg, Cu, and Be ($r < 0.25$), indicating they had different sources. Numerous studies have demonstrated that Cd, As, and Pb are associated with industrial and urban pollution in riverine areas (Proshad et al., 2022; Li et al., 2022). An early study conducted in the Yangtze River basin showed that HM pollution was mainly from electroplating, metal processing, and industrial wastewater (Yi et al., 2011). A recent study also suggested that high Cd concentrations in Lake Tai sediments were mainly produced in industrial processes (Niu et al., 2020). In this study, Cd was identified as the priority pollutant. Not strangely, the study area has been known as the ceramic capital of China, relying on raw materials rich in high levels of Cd, such as pigments (Cd red and Cd yellow) (ATSDR, 2012). According to the Yixing Yearbook in 2022, the electroplating (e.g., wire and cable industries) and metal materials industries were dominant in terms of sales revenue, accounting for more than 40% of the city's industrial economy. These were pillar and traditional industries in Yixing city, which were built along the Nanxi River to take full advantage of the favorable locations and conditions. With the rapid industrial and economic development in the plain river networks, the violation and noncompliance discharges of industrial wastewater brought about Cd, Pb, As, and Zn leakage and contamination in river system (Xia et al., 2020; Luo et al., 2021; Jiang et al., 2021). Hence, factor 2 was determined as industrial discharges.

Factor 3 was dominated by Cu (38.4%), Zn (17.4%), and Ni (16.8%), which in combination corresponds to the significant positive correlations ($0.83 < r < 0.87$, $p < 0.05$), indicating that these metals had similar sources and/or geochemical behaviors (Proshad et al., 2022). Atmospheric deposition is one of the most important pathways for heavy metal pollution in water (Zhou et al., 2020). The activities of energy, transport, metallurgy, and construction materials carry large quantities of HMs such as Cu, Zn and Ni, which are released in the form of drifting dust, ash, particulate or gas, and finally deposited into water via dry and wet deposition (Guo et al., 2021). Some recent studies further found that Cu after atmospheric deposition had high mobility with an obvious enrichment effect on crops, thus posing a threat to the quality of food products, at least in regions where substantial atmospheric heavy metal deposition was emerging (Zhou et al., 2020; Liu et al., 2022). In the study, the sites with high contents of Cu, Zn, and Ni were mostly concentrated in the city center, especially in commercial and residential areas with dense traffic routes (Fig. 2c and Fig. S2). Additionally, the content distributions of these metals showed an overall increasing trend from northwest to southeast. This was probably due to the increase in coal combustion in winter, and thus the gradual accumulation and deposition of pollutants transported to the atmosphere under the action of the local winter monsoon (northwesterly wind) (Li et al., 2018). Similar findings by Li et al. (2018) implied that the concentration of Zn from atmospheric dustfall was higher in winter than in summer in western Lake Tai sediments. As analyzed above, the factor was classified as atmospheric deposition.

Factor 4 was weighted by Be (74.3%), V (64.7%), Cr (56.6%), and Co (56.1%), which was confirmed by their significant associations ($0.84 < r < 0.95$, $p < 0.05$), reflecting they probably had the same pollution source. There were no distinct spatial patterns in Be and V distributions, with the lowest coefficient variations being 21.2% and 20.0%, respectively. Additionally, the contents of these metals were close to their background values, indicating that they primarily came from the natural environment with less human interference (Xia et al., 2020). The findings were further confirmed by previous studies that Be, V, Cr, and Co could deposit into river sediments during exogenic geological processes, such as rock weathering (Proshad et al., 2022), the erosion of riverbeds, and the dissolution of minerals (Sheng et al., 2022). Thus, Factor 4 was mostly influenced by the natural background.

As a whole, industrial discharges, agricultural activities, and atmospheric deposition were identified as anthropogenic factors of HMs, with the contributions of 37.0%, 12.2%, and 8.0%, respectively. Spatially, agricultural and industrial sources had tremendous geographic variances. The midstream river ran through the city center with an agglomeration of intensive industrial and urban activities, where industrial discharges (factor 2) were mostly concentrated. The agricultural activities (factor 1) were mainly dispersed in the downstream river near Lake Tai, where grew rice, wheat and rape. Many industries have been established and well-developed along the Nanxi River, such as the electroplating, textile, ceramics, mining, battery, and steel manufacturing industries (Chen et al., 2021a; Li et al., 2022). The primary, secondary, and tertiary industries increased by 2.87%, 51.02%, and 46.11% in Yixing city, respectively (Yixing Yearbook). Accordingly, industrial discharges are supposed to attract much attention with reasonable adjustment and optimization.

3.3. Comparison of Unmix with PMF for source apportionment of sedimental metals

Comparatively, we further performed the Unmix model for source apportionment of sedimental metals. The PMF and Unmix models were compared and analyzed. In the study, four sources were also extracted by the Unmix with the RSQ value of 0.96 (>0.8) and the S/N value of 2.07 (>2); thereby the analytical results of source apportionment were reliable. The metal Hg was suggested to be excluded by the Unmix. However, Hg was identified as a main contaminant, and its specific variance (61%) was only a little more than 50%. Therefore, it was not excluded herein (U.S. EPA, 2007). A positive linear correlation of the source contribution rates between PMF and Unmix was found with good consistency ($r = 0.80$, $p < 0.05$) (Fig. S4). Overall, the two models obtained similar results for the factor profiles and contributions with reasonable prediction efficacy.

Unmix model showed the average contributions in the order of natural source (42.9%) > industrial discharges (32.3%) > atmospheric deposition (15.8%) > agricultural activities (8.9%), which was in line with the source apportionment results of the PMF model (Fig. S5). The anthropogenic factor (57.1%) was apportioned as the most significant contribution factor to influence the concentrations and distributions of sedimental metals. Among them, the industrial discharge was the primary source contribution (32.3%–37.0%), followed by atmospheric deposition (12.1%–15.9%) and agricultural activity (8.0%–9.0%). The results were consistent with the study by Chen et al. (2019a), who proposed that industrial activities contributed more than half (53%) in Lake Tai basin. According to the Yixing Yearbook (http://www.yxdaszg.cn/), the study area has experienced remarkable economic development, with the annual growth rates of GDP, urbanization and population being 15.7%, 9.2% and 3.0% over the past 30 years, respectively (Xu et al., 2016). As one of the biggest comprehensive industrial bases in China, the study area discharged large amounts of pollutants into the water environment (Chen et al., 2021a; Luo et al., 2021). The levels of HMs have continuously increased and accumulated in soil via processes of complexation or oxidation, and then deposited in river sediments via surface and subsurface runoff (Li et al., 2020; Li et al., 2021).

Interestingly, differences were also found between the PMF and Unmix models for the source apportionment of sediment metals (Fig. 3a vs Fig. 3c). An intra-comparison with the regression results of predicted and observed data concentrations of HMs could evaluate the model performance. Herein, the values of r^2 varied from 0.67 to 0.98 in the Unmix and from 0.54 to 0.99 in the PMF, showing both models fitted all

the HMs in well. Notably, there were some zero values (<1%) in the source component spectrum by the Unmix, and its edges were not well-defined and straight. Hence, it was assumed that the results by PMF were more reliable. Previously, similar findings were also reported by Henry and Christensen. (2010) and Diakite et al. (2021) that the data did not support reliable Unmix results due to unclear edges. Nevertheless, the Unmix fitted better in some elements. For example, the r^2 for Cd was 0.98 in the Unmix, which was higher than that (0.54) in the PMF. Therefore, the two models can support each other to minimize the potential weaknesses of individual models and thereby get more convincing conclusions (Salim et al., 2019). Notably, this paper did some exploratory work in comparison of receptor models, which further needs long-term monitoring and practice. Regardless, the framework has important implications for providing a comprehensive understanding of HM risk and their sources in plain rivers.

3.4. Source-specific ecological risks posed by sedimental metals

The apportionment results of PMF and Unmix models were further combined and used for characterizing the source-oriented ecological risks of HMs in river sediments. The concentration fraction of sediment metals extracted from the two models were integrated into the modified ecological risk model. Additionally, the ecological risks of HMs for the measured concentration were calculated, i.e., the total factors. Table 2 shows the ratio of class distributions for the modified ecological risk index of HMs from the four identified sources and the total factors. For the total factors (measured concentrations), the *RI* index showed that 78% and 20% of the sampling sites were found to be high and considerable risks, respectively. Notably, Cd and Hg posed an extremely high ecological risk at approximately 80% and 34% of the sampling sites, and a high ecological risk at 16% and 58% of the sampling sites, respectively. In addition, 96% and 58% of the sampling sites caused by Cd and Hg contributed to extreme ecological risks, respectively. The two metals could be easily deposited and carried by sediments due to their relatively lower concentration product (*Ksp*), resulting in high ecological risks (Li et al., 2018; Luo et al., 2021). Xia et al. (2020) also proposed that the high exchangeable fraction of Cd made it more prone to high risks.

The source-specific ecological risks from the four identified sources varied considerably. The considerable and high risks caused by agricultural activities accounted for 60% and 30%, respectively. Although both PMF and Unmix models revealed that natural sources had the highest contribution to HMs, industrial discharges made higher percentages on the high-(52%) and extreme-(36%) risk of sediment metals. Specifically, natural sources accounted for more than 52% of the moderate or below risks, while they only contributed very little to high or extreme risks (<10%). Industrial discharge was not considered the highest proportion for the total accumulation of HMs, but it was the largest contributor to the ecological risk. As a whole, the contributions of the four sources to sediment HMs were not in accordance with the results of source-specific risks, which was confirmed by previous studies (Men et al., 2020; Li et al., 2021). Therefore, a comprehensive understanding of source-specific risk apportionment analysis is significant for effective source control and treatment (Fei et al., 2022; Yan et al., 2022).

Notably, Cd and Hg were also found to be crucial elements posing serious ecological risks from specific sources. The Cd pollution caused by industrial discharges posed high-(44%) and extreme-(52%) risks, and the Hg contamination produced from agricultural activities mainly contributed to considerable-(36%) and high-(46%) risks. The results also fitted well with previous findings that Cd and Hg metals posed greater ecological risks than other studied metals (Liu et al., 2018; Men et al., 2020; Niu et al., 2020). Additionally, it was reported that Cd was a severe threat to most lake sediments (99%) along the Yangtze River (Luo et al., 2021). In this study, Hg showed a higher level near Lake Tai, which was consistent with Chen et al. (2019a). Therefore, to protect China's third-largest freshwater lake, priority should be given to the control and treatment of Cd and Hg pollution from industrial and agricultural sources.

Further, we calculated the $mNIER^k$ value (k = 1, 2, 3, 4) to reflect the contribution of four identified sources to ecological risks (Fig. 4a). In spatial, *mNIER* was significantly influenced by industrial discharges from regions on the eastern side near Lake Tai and the city center, posing the highest ecological risk among specific sources. Relatively, the lower ecological risk was derived from agricultural activities with smaller fluctuation than industrial discharges. Notably, the spatial variation of *mNIER* for agricultural activities showed an opposite regional trend to that for industrial discharges; that was, the regional minimum value of *mNIER* induced by agricultural source was often the regional maximum value of *mNIER* caused by industrial source. However, the spatial similarity was that the overall trend was lower upstream than downstream. This might be closely related to district site selections of agriculture and industry. The lower values of *mNIER* from atmospheric deposition and natural sources (<80) suggested relatively limited ecological risks posed by the two sources. Overall, source-specific ecological risks with *mNIER* followed the order of industrial discharges > agricultural activities > natural sources > atmospheric deposition (Fig. 4b). The results indicated that the anthropogenic sources of HMs were expected to be attached to great importance, and similar findings were also reported in the Pearl River (Xiao et al., 2022), Yellow River (Wang et al., 2022a), Jiulong River (Yan et al., 2022), and Fenhe River (Wang et al., 2022b) of China. Therefore, anthropogenic activities should be prioritized and optimized to mitigate HMs pollution and protect the river ecosystem.

3.5. Antibiotic resistome risk and its association with source-oriented geochemical enrichment of sedimental metals

In the river sediments, 212 ARGs were identified through high-throughput sequencing-based metagenomic assembly analysis, most of which were not previously detected using culture-dependent approaches and/or qPCR methods in this area (Stange et al., 2019). These ARGs belong to 21 types and confer resistance to the commonly used antibiotics (i.e., bacitracin, quinolones, and polymyxin) (Fig. 5a). Among them, the most abundant ARG type was multidrug resistance genes, followed by macrolide-lincosamide-streptogramin (MLS) and quinolone resistance genes with abundances of 101.75, 78.11 and 16.38 × /Gb,

Table 2
Ratio of class distribution for the modified ecological risk index of heavy metals from the total factors and the potential four sources identified by PMF and Unmix models.

	Low	Moderate	Considerable	High	Extremely high
Total factors					
Cr	100%	0%	0%	0%	0%
Cd	0%	0%	2%	2%	96%
As	100%	0%	0%	0%	0%
Hg	0%	0%	2%	40%	58%
Pb	100%	0%	0%	0%	0%
Cu	100%	0%	0%	0%	0%
Zn	100%	0%	0%	0%	0%
Ni	100%	0%	0%	0%	0%
Mn	100%	0%	0%	0%	0%
V	100%	0%	0%	0%	0%
Be	100%	0%	0%	0%	0%
Co	100%	0%	0%	0%	0%
Industrial discharges					
Cd	0%	2%	2%	44%	52%
Hg	78%	22%	0%	0%	0%
Agricultural activities					
Cd	98%	2%	0%	0%	0%
Hg	0%	4%	36%	46%	14%
Atmospheric deposition					
Cd	100%	0%	0%	0%	0%
Hg	100%	0%	0%	0%	0%
Natural source					
Cd	8%	48%	36%	6%	2%
Hg	100%	0%	0%	0%	0%

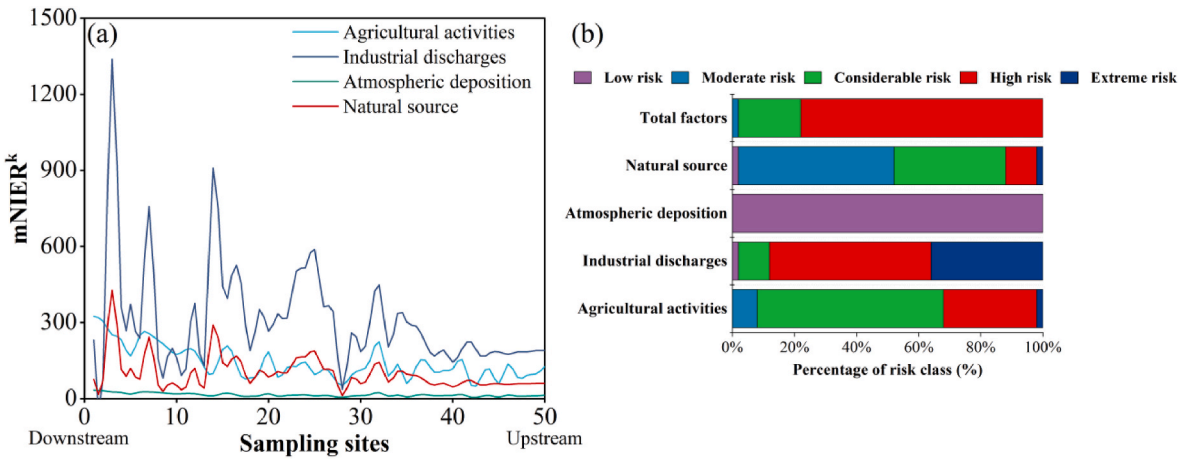

Fig. 4. Source-oriented ecological risk of metals in the river sediments. **(a)** The distribution of modified Nemerow integrated ecological risk (mNIER) in the river sediments posed by heavy metals from the four apportioned sources; **(b)** Percentages of the class distribution of ecological risk posed by heavy metals for the identified four sources and the total factors (measured concentration).

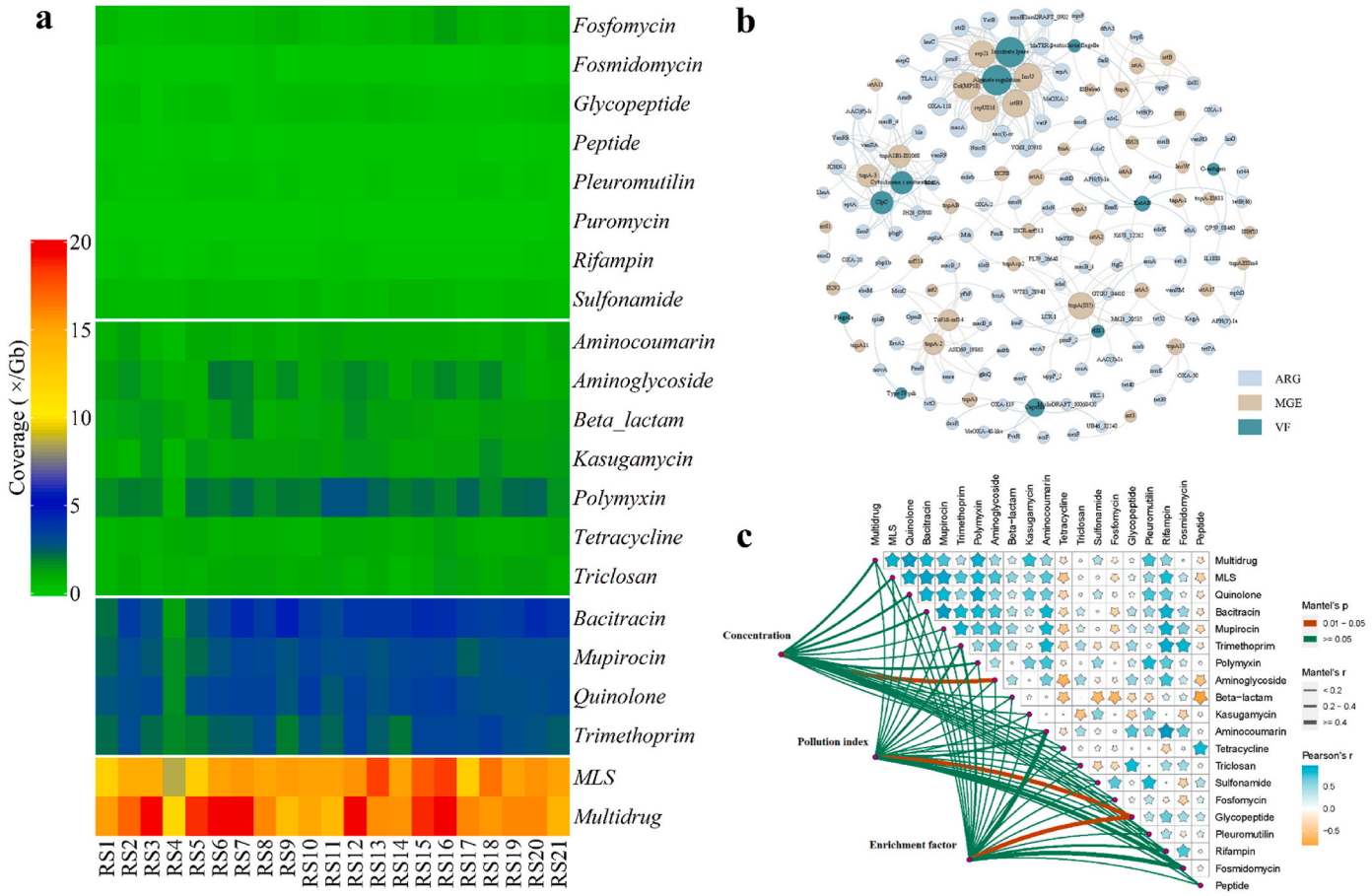

Fig. 5. Antibiotic resistome risk and its association with geochemical enrichment of heavy metals in the river sediments. **a.** Profiles of the antibiotic resistance genes (ARGs) in the sediment metagenomes (× /Gb) (MLS: macrolide-lincosamide-streptogramin); **b.** Network analysis revealing the co-occurrence of ARGs with mobile genetic elements (MGEs) and virulence factor genes (VFGs) based on their robust and significant correlations (Spearman's correlation coefficient $\rho > 0.8$; P-value <0.01). The size of each node is proportional to the number of connections; **c.** Mantel analysis showing the relationship of ARGs with the geochemical enrichment of heavy metals in the river sediments.

respectively. These top 3 ARG types had strong correlations with the total coverage of ARGs ($p < 0.05$) and occupied 65–71% of the total ARGs for each sample. Not strangely, multidrug resistance genes have also been reported previously to be the most dominant ARG types owing to the ubiquity of prokaryotic multidrug resistance efflux pumps in aquatic environments (Chen et al., 2019b). Various multidrug-ARGs in the environment were closely related to the widespread use of diverse antibiotics in human medicine, livestock therapy, and growth promotion (Zhang et al., 2015). Notably, some emerging genes were also found in the river sediments, including *mcr*-type (i.e., mcr-4 and mcr-5) and

carbapenem-resistance genes (i.e., OXA- and KPC-type). These emerging ARGs could make bacteria resistant to colistin and carbapenem which are the last-resort drugs, making it more difficult to treat infections with resistant pathogens, thus resulting in high resistome risks (Liu et al., 2016).

Regarding the spread risk of ARGs, a resistance readiness condition system was developed by Martínez et al. (2015), who suggested that ARGs presenting on MGEs in human pathogens were assigned a high transmission risk. Generally, MGEs are considered as the main carriers of ARGs and facilitate the horizontal transfer of ARGs (Wang et al., 2021). Herein, a total of 69 MGEs were identified in river sediments (Fig. S6), of which *tnpA*, *IS91*, and *intI1* were more abundant than others. Previous studies showed that *tnpA* (transposase) played an important role in ARG transmission, and *intI1* (integrase) was a human activity marker with high abundance in diverse environments (Gillings et al., 2015). Also, by comparing the pathogenic bacteria database (Li et al., 2015) and virulence factor database (Zhang et al., 2022a), we identified 335 human bacterial pathogens (HBPs) species and 24 virulence factor genes (VFGs) in the river sediments (Fig. S7). The VFGs enhance pathogen invasion making the organism immunity to bacterial infection (Durso et al., 2011). More importantly, MGEs could carry VFGs for horizontal genetic transmission, increasing pathogenic bacteria in environments (Zhang et al., 2022a, 2022b). Further, the co-occurrence of ARGs, VFGs, and MGEs was explored to identify the potential resistome transmission risks (Fig. 5b). Results showed that more ARGs mainly belonging to beta-lactam, MLS, aminoglycoside, multidrug, polymyxin, glycopeptide, bacitracin, tetracycline resistance genes, had significant correlations with multiple MGEs and VFGs ($\rho > 0.8$; P-value <0.01), indicating strong propagation risk of ARGs in the environment (Martínez et al., 2015).

Regarding the association of resistome risk with the geochemical enrichment of HMs in environments, a growing number of research suggested that HMs could significantly affect the prevalence and spread of ARGs (Baker-Austin et al., 2006; Ji et al., 2012; Xu et al., 2017). In the study, network analysis displayed more metals were closely associated with multiple ARGs, suggesting the potential impact of HMs on ARGs in environments. Especially, the highly contaminated Cd and Cu in river sediments had a strong correlation with more ARGs such as *mepB* (multidrug), *tetB(P)* (tetracycline), *oleC* (MLS), *OXA-3* (beta_lactam) and *vanRM* (glycopeptide). Also, our analyses identified 56 heavy metal resistance genes (HMRGs) in the river sediments, including Cd, Cu, As, Hg, Cr, Zn, Co, and Ni resistance genes, as well as their symbiotic modes with ARGs ($\rho > 0.8$; P-value <0.01) (Fig. S8). As shown in Fig. S9, *arsA* (As), *arsB* (As), *cadC* (Cd, Zn), and *merT* (Hg) resistance genes are significantly related to many ARGs (>15).

Mantel test analysis further showed a significant strong correlation ($p < 0.05$) between some ARGs (i.e., aminoglycoside and glycopeptide) and the enrichment factor of HMs in river sediments (Fig. 5c). Herein, we employed the enrichment factor of HMs since the index could measure the influence of anthropogenic activities (Zhang et al., 2022a). The results suggested that HMs exerted co-selective pressure on antibiotic-resistant groups in the environment. Also, we explored associations of ARGs with the source-oriented geochemical enrichment of HMs in the environment. The geochemical enrichments of HMs from agricultural activities, industrial discharge, atmospheric deposition, and natural background had weak correlations with ARGs (Fig. S10). The findings implied that the antibiotic resistance in the environment may be determined by selective pressure from more factors rather than a single source. Nevertheless, the wide prevalence of ARGs and their co-occurrences with HMRGs in the river sediments suggested the development, evolution, and spread of antibiotic resistance even when bacteria became resistant to HMs, which was also confirmed by the coexistence analysis between ARGs and HMs in the environment. Previous investigations also discovered the HM risks on the prevalence and spread of ARGs in environments even in low contamination levels (Chen et al., 2021a, 2021b). It should be noted that, although our analyses have suggested that the geochemical enrichment of HMs may increase antibiotic resistiome risks, the effects of HMs on the evolution and spread of ARGs must be further explored using more molecular approaches, such as culture-based and/or functional genomic methods. Regardless, our results can raise concerns about metal-driven antibiotic resistance among the scientific community, the government, and the public.

4. Conclusion

The study proposed a new integrated technological framework to characterize the source-oriented ecological and resistome risks associated with the geochemical enrichment of HMs in river sediments. The geochemical contamination analyses indicated Cd, Hg, Zn, and Cu were the major contaminants with significant risk levels, with 19.7, 7.5, 2.9, and 2.2 times higher than their background values, respectively. The apportionment results suggested that Cd and Hg were mainly derived from industrial discharges and agricultural activities, respectively, while Cu and Zn were mainly characterized by atmospheric deposition. Averagely, the source contributions were 42.9%, 34.7%, 14.0%, and 8.5% for natural background, industrial discharges, atmospheric deposition, and agricultural activities, respectively. The source-oriented ecological risk assessment further showed that industrial and agricultural activities largely determined the ecological risks posed by HMs. Furthermore, abundant and diverse ARGs were identified in river sediments, and significant correlations were discovered between the ARGs and enrichment factors of HMs in the environment. To protect the third largest freshwater lake of China, priority should be given to the discharge control of Cd and Hg especially from industrial and agricultural activities.

Author contributions statement

Zhimin Yang: Methodology, Data curation, Formal analysis, Visualization, Writing – original draft. **Chunhui Li**: Methodology, Formal analysis, Writing – review & editing. **Haiyang Chen***: Resources, Validation, Writing – review & editing. **Xin Shan**: Data curation. **Jinping Chen**: Sample collection and processing. **Jianhang Zhang**: Sample collection and processing. **Shaoda Liu***: Validation, Writing – review & editing, Supervision. **Qiang Liu**: Investigation. **Xuan Wang**: Writing – review & editing.

Declaration of competing interest

The authors declare that they have no known competing financial interests or personal relationships that could have appeared to influence the work reported in this paper.

Data availability

Data will be made available on request.

Acknowledgments

This work was supported by the National Key Research and Development Program of China (2022YFC3202001) and the National Natural Science Foundation of China (52070023).

Appendix A. Supplementary data

Supplementary data to this article can be found online at https://doi.org/10.1016/j.chemosphere.2023.139119.

References

Agency for Toxic Substances and Diseases Registry (ATSDR), 2012. Toxicological Profile for Cadmium. https://www.atsdr.cdc.gov/toxprofiledocs/index.html?id=48&tid=15.

Baker-Austin, C., Wright, M.S., Stepanauskas, R., McArthur, J.V., 2006. Co-selection of antibiotic and metal resistance. Trends Microbiol. 14, 176–182. https://doi.org/10.1016/j.tim.2006.02.006.

Chen, R., Chen, H., Song, L., Yao, Z., Meng, F., Teng, Y., 2019a. Characterization and source apportionment of heavy metals in the sediments of Lake Tai (China) and its surrounding soils. Sci. Total Environ. 694, 133819 https://doi.org/10.1016/j.scitotenv.2019.133819.

Chen, H., Bai, X., Li, Y., Jing, L., Chen, R., Teng, Y., 2019b. Source identification of antibiotic resistance genes in a peri-urban river using novel crAssphage marker genes and metagenomic signatures. Water Res. 167, 115098 https://doi.org/10.1016/j.watres.2019.115098.

Chen, R., Zhang, Q., Chen, H., Yue, W., Teng, Y., 2021a. Source apportionment of heavy metals in sediments and soils in an interconnected river-soil system based on a composite fingerprint screening approach. J. Hazard Mater. 411, 125125 https://doi.org/10.1016/j.jhazmat.2021.125125.

Chen, H., Liu, C., Teng, Y., Zhang, Z., Chen, Y., Yang, Y., 2021b. Environmental risk characterization and ecological process determination of bacterial antibiotic resistome in lake sediments. Environ. Int. 147, 106345 https://doi.org/10.1016/j.envint.2020.106345.

Durso, L., Harhay, G., Bono, J., Smith, T., 2011. Virulence-associated and antibiotic resistance genes of microbial populations in cattle feces analyzed using a metagenomic approach. J. Microbiol. Methods 84 (2), 278–282. https://doi.org/10.4172/2325-9590.1000134.

Diakite, M., Hu, Y., Cheng, H., 2021. Source apportionment based on the comparative approach of two receptor models in a large-scale region in China. Environ. Sci. Pollut. Res. 28 (40), 56696–56710. https://doi.org/10.1007/s11356-021-14602-1.

Fan, H., Chen, S., Li, Z., Liu, P., Xu, C., Yang, X., 2020. Assessment of heavy metals in water, sediment and shellfish organisms in typical areas of the Yangtze River Estuary, China. Mar. Pollut. Bull. 151, 110864 https://doi.org/10.1016/j.marpolbul.2019.110864.

Fei, X., Lou, Z., Xiao, R., Ren, Z., Lv, X., 2022. Source analysis and source-oriented risk assessment of heavy metal pollution in agricultural soils of different cultivated land qualities. J. Clean. Prod. 341, 130942 https://doi.org/10.1016/j.jclepro.2022.130942.

Gillings, M., Gaze, W., Pruden, A., Smalla, K., Tiedje, J., Zhu, Y., 2015. Using the class 1 integron-integrase gene as a proxy for anthropogenic pollution. ISME J. 9, 1269–1279. https://doi.org/10.1038/ismej.2014.226.

Guo, X., Sun, Q., Zhao, Y., Cai, H., 2019. Identification and characterisation of heavy metals in farmland soil of Hunchun basin. Environ. Earth Sci. 78, 310. https://doi.org/10.1007/s12665-019-8314-0.

Gu, X., Xu, L., Wang, Z., Ming, X., Dang, P., Ouyang, W., Lin, C., Liu, X., He, M., Wang, B., 2021. Assessment of cadmium pollution and subsequent ecological and health risks in Jiaozhou Bay of the Yellow Sea. Sci. Total Environ. 774, 145016 https://doi.org/10.1016/j.scitotenv.2021.145016.

Guo, G., Wang, Y., Zhang, D., Lei, M., 2021. Source-specific ecological and health risks of potentially toxic elements in agricultural soils in Southern Yunnan Province and associated uncertainty analysis. J. Hazard Mater. 417, 126144 https://doi.org/10.1016/j.jhazmat.2021.126144.

Hakanson, L., 1980. An ecological risk index for aquatic pollution control a sedimentological approach. Water Res. 14 (8), 975–1001. https://doi.org/10.1016/0043-1354(80)90143-8.

Henry, R., Christensen, E., 2010. Selecting an appropriate multivariate source apportionment model result. Environ. Sci. Technol. 44, 2474–2481. https://doi.org/10.1021/es9018095.

Huang, Y., Li, T., Wu, C., He, Z., Japenga, J., Deng, M., Yang, X., 2015. An integrated approach to assess heavy metal source apportionment in peri-urban agricultural soils. J. Hazard Mater. 299, 540–549. https://doi.org/10.1016/j.jhazmat.2015.07.041.

Huang, C., Cai, L., Xu, Y., Wen, H., Jie, L., Hu, G., Chen, L., Wang, H., Xu, X., Mei, J., 2022a. Quantitative analysis of ecological risk and human health risk of potentially toxic elements in farmland soil using the PMF model. Land Degrad. Dev. 33 (11), 1954–1967. https://doi.org/10.1002/ldr.4277.

Huang, C., Cai, L., Xu, Y., Jie, L., Chen, L., Hu, G., Jiang, H., Xu, X., Mei, J., 2022b. A comprehensive exploration on the health risk quantification assessment of soil potentially toxic elements from different sources around large-scale smelting area. Environ. Monit. Assess. 194 (3) https://doi.org/10.1007/s10661-022-09804-0.

Ji, X., Shen, Q., Liu, F., Ma, J., Xu, G., Wang, Y., Wu, M., 2012. Antibiotic resistance gene abundances associated with antibiotics and heavy metals in animal manures and agricultural soils adjacent to feedlots in Shanghai; China. J. Hazard Mater. 235–236, 178–185. https://doi.org/10.1016/j.jhazmat.2012.07.040.

Jiang, H., Cai, L., Hu, G., Wen, H., Luo, J., Xu, H., Chen, L., 2021. An integrated exploration on health risk assessment quantification of potentially hazardous elements in soils from the perspective of sources. Ecotoxicol. Environ. Saf. 208, 111489 https://doi.org/10.1016/j.ecoenv.2020.111489.

Keeler, G., Landis, M., Norris, G., Christianson, E., Dvonch, J., 2006. Sources of mercury wet deposition in eastern Ohio, USA. Environ. Sci. Technol. 40, 5874–5881. https://doi.org/10.1021/es060377q.

Li, B., Ju, F., Cai, L., Zhang, T., 2015. Profile and fate of bacterial pathogens in sewage treatment plants revealed by high-throughput metagenomic approach. Environ. Sci. Technol. 49 (17), 10492–10502. https://doi.org/10.1021/acs.est.5b02345.

Liu, Y., Wang, Y., Walsh, T., Yi, L., Zhang, R., Spencer, J., Doi, Y., Tian, G., Dong, B., Huang, X., Yu, L., Gu, D., Ren, H., Chen, X., Lv, L., He, D., Zhou, H., Liang, Z., Liu, J., Shen, J., 2016. Emergence of plasmid-mediated colistin resistance mechanism MCR-1 in animals and human beings in China: a microbiological and molecular biological study. Lancet Infect. Dis. 16, 161–168. https://doi.org/10.1016/S1473-3099(15)00424-7.

Li, R., Tang, C., Cao, Y., Jiang, T., Chen, J., 2018. The distribution and partitioning of trace metals (Pb, Cd, Cu, and Zn) and metalloid (As) in the Beijiang River. Environ. Monit. Assess. 190 (7), 399. https://doi.org/10.1007/s10661-018-6789-x.

Liu, J., Chen, Y., Chao, S., Cao, H., Zhang, A., Yang, Y., 2018. Emission control priority of PM2. 5-bound heavy metals in different seasons: a comprehensive analysis from health risk perspective. Sci. Total Environ. 644, 20–30. https://doi.org/10.1016/j.scitotenv.2018.06.226.

Li, Y., Chen, H., Teng, Y., 2020. Source apportionment and source-oriented risk assessment of heavy metals in the sediments of an urban river-lake system. Sci. Total Environ. 737, 140310 https://doi.org/10.1016/j.scitotenv.2020.140310.

Li, Y., Chen, H., Song, L., Wu, J., Sun, W., Teng, Y., 2021. Effects on microbiomes and resistomes and the source-specific ecological risks of heavy metals in the sediments of an urban river. J. Hazard Mater. 409, 124472 https://doi.org/10.1016/j.jhazmat.2020.124472.

Luo, M., Yu, H., Liu, Q., Lan, W., Ye, Q., Niu, Y., Niu, Y., 2021. Effect of river-lake connectivity on heavy metal diffusion and source identification of heavy metals in the middle and lower reaches of the Yangtze River. J. Hazard Mater. 416, 125818 https://doi.org/10.1016/j.jhazmat.2021.125818.

Li, Y., Cheng, X., Liu, K., Yu, Y., Zhou, Y., 2022. A new method for identifying potential hazardous areas of heavy metal pollution in sediments. Water Res. 224, 119065 https://doi.org/10.1016/j.watres.2022.119065.

Liu, X., Wang, H., Li, L., Deng, C., Chen, Y., Ding, H., Yu, Z., 2022. Do microplastic biofilms promote the evolution and co-selection of antibiotic and metal resistance genes and their associations with bacterial communities under antibiotic and metal pressures? J. Hazard Mater. 424, 127285 https://doi.org/10.1016/j.jhazmat.2021.127285.

Martínez, J., Coque, T., Baquero, F., 2015. What is a resistance gene? Ranking risk in resistomes. Nat. Rev. Microbiol. 13, 116. https://doi.org/10.1038/nrmicro3399.

Men, C., Liu, R., Xu, L., Wang, Q., Guo, L., Miao, Y., Shen, Z., 2020. Source-specific ecological risk analysis and critical source identification of heavy metals in road dust in Beijing. China. J. Hazard Mater. 388, 121763 https://doi.org/10.1016/j.jhazmat.2019.121763.

Men, C., Liu, R., Wang, Q., Miao, Y., Wang, Y., Jiao, L., Li, L., Cao, L., Shen, Z., Li, Y., Crawford-Brown, D., 2021. Spatial-temporal characteristics, source-specific variation and uncertainty analysis of health risks associated with heavy metals in road dust in Beijing, China. Environ. Pollut. 278, 116866.

Magesh, N., Tiwari, A., Botsa, S., da Lima Leitao, T., 2021. Hazardous heavy metals in the pristine lacustrine systems of Antarctica: insights from PMF model and ERA techniques. J. Hazard Mater. 412, 125263 https://doi.org/10.1016/j.jhazmat.2021.125263.

Niu, Y., Jiang, X., Wang, K., Xia, J., Jiao, W., Niu, Y., Yu, H., 2020. Meta analysis of heavy metal pollution and sources in surface sediments of Lake Taihu, China. Sci. Total Environ. 700, 134509 https://doi.org/10.1016/j.scitotenv.2019.134509.

Ouyang, W., Jiao, W., Li, X., Giubilato, E., Critto, A., 2016. Long-term agricultural non-point source pollution loading dynamics and correlation with outlet sediment geochemistry. J. Hydrol. 540, 379–385. https://doi.org/10.1016/j.jhydrol.2016.06.043.

Proshad, R., Kormoker, T., Al, M., Islam, M., Khadka, S., Idris, A., 2022. Receptor model-based source apportionment and ecological risk of metals in sediments of an urban river in Bangladesh. J. Hazard Mater. 423, 127030 https://doi.org/10.1016/j.jhazmat.2021.127030.

Stange, C., Yin, D., Xu, T., Guo, X., Schäfer, C., Tiehm, A., 2019. Distribution of clinically relevant antibiotic resistance genes in Lake Tai, China. Sci. Total Environ. 655, 337–346. https://doi.org/10.1016/j.scitotenv.2018.11.211.

Salim, I., Sajjad, R., Paule-Mercado, M., Memon, S., Lee, B., Sukhbaatar, C., Lee, C., 2019. Comparison of two receptor models PCA-MLR and PMF for source identification and apportionment of pollution carried by runoff from catchment and sub-watershed areas with mixed land cover in South Korea. Sci. Total Environ. 663, 764–775. https://doi.org/10.1016/j.scitotenv.2019.01.377.

Shi, X., Nenes, A., Xiao, Z., Song, S., Yu, H., Shi, G., Zhao, Q., Chen, K., Feng, Y., Russell, A., 2019. High-resolution data sets unravel the effects of sources and meteorological conditions on nitrate and its gas-particle partitioning. Environ. Sci. Technol. 53 (6), 3048–3057. https://doi.org/10.1021/acs.est.8b06524.

Sheng, D., Meng, X., Wen, X., Wu, J., Yu, H., Wu, M., 2022. Contamination characteristics, source identification, and source-specific health risks of heavy metal (loid)s in groundwater of an arid oasis region in Northwest China. Sci. Total Environ. 841, 156733 https://doi.org/10.1016/j.scitotenv.2022.156733.

U.S. Environmental Protection Agency, 2007. EPA Unmix 6.0 Fundamentals & User Guide. https://www.epa.gov/air-research/epa-unmix-60-fundamentals-user-guide.

U.S. Environmental Protection Agency, 2014. EPA Positive Matrix Factorization (PMF) 5.0 Fundamentals & User Guide. https://www.epa.gov/air-research/forms/registration-download-and-use-epa-pmf-50.

UNEP, 2017. Frontiers 2017 Emerging Issues of Environmental Concern. United Nations Environment Programme, Nairobi.

Wang, Y., Yang, L., Kong, L., Liu, E., Wang, L., Zhu, J., 2015. Spatial distribution, ecological risk assessment and source identification for heavy metals in surface sediments from Dongping Lake, Shandong, East China. Catena 125, 200–205. https://doi.org/10.1016/j.catena.2014.10.023.

Wang, X., Lan, B., Fei, H., Wang, S., Zhu, G., 2021. Heavy metal could drive co-selection of antibiotic resistance in terrestrial subsurface soils. J. Hazard Mater. 411, 124848 https://doi.org/10.1016/j.jhazmat.2020.124848.

Wang, L., Wang, Y., Li, H., Zhu, Y., Liu, R., 2022a. Occurrence, source apportionment and source-specific risk assessment of antibiotics in a typical tributary of the Yellow River basin. J. Environ. Manag. 305, 114382 https://doi.org/10.1016/j.jenvman.2021.114382.

Wang, Y., Wang, L., Liu, R., Li, L., Cao, L., Jiao, L., Xia, X., 2022b. Source-specific risk apportionment and critical risk source identification of antibiotic resistance in Fenhe River basin, China. Chemosphere 287, 131997. https://doi.org/10.1016/j.chemosphere.2021.131997.

Xu, J., Guo, J., Liu, G., Shi, G., Guo, C., Zhang, Y., Feng, Y., 2014. Historical trends of concentrations, source contributions and toxicities for PAHs in dated sediment cores from five lakes in western China. Sci. Total Environ. 470, 519–526. https://doi.org/10.1016/j.scitotenv.2013.10.022.

Xu, X., Yang, G., Tan, Y., Zhuang, Q., Li, H., Wan, R., Su, W., Zhang, J., 2016. Ecological risk assessment of ecosystem services in the Taihu Lake Basin of China from 1985 to 2020. Sci. Total Environ. 554–555, 7–16. https://doi.org/10.1016/j.scitotenv.2016.02.120.

Xu, Y., Xu, J., Mao, D., Luo, Y., 2017. Effect of the selective pressure of sub-lethal level of heavy metals on the fate and distribution of ARGs in the catchment scale. Environ. Pollut. 220, 900–908. https://doi.org/10.1016/j.envpol.2016.10.074.

Xia, F., Zhang, C., Qu, L., Song, Q., Ji, X., Mei, K., Zhang, M., 2020. A comprehensive analysis and source apportionment of metals in riverine sediments of a rural-urban watershed. J. Hazard Mater. 381, 121230 https://doi.org/10.1016/j.jhazmat.2019.121230.

Xia, F., Niu, X., Qu, L., Dahlgren, R.A., Zhang, M., 2021. Integrated source-risk and uncertainty assessment for metals contamination in sediments of an urban river system in eastern China. Catena 203, 105277. https://doi.org/10.1016/j.catena.2021.105277.

Xiao, H., Shahab, A., Ye, F., Wei, G., Li, J., Deng, L., 2022. Source-specific ecological risk assessment and quantitative source apportionment of heavy metals in surface sediments of Pearl River Estuary, China. Mar. Pollut. Bull. 179, 113726 https://doi.org/10.1016/j.marpolbul.2022.113726.

Yi, Y., Yang, Z., Zhang, S., 2011. Ecological risk assessment of heavy metals in sediment and human health risk assessment of heavy metals in fishes in the middle and lower reaches of the Yangtze River basin. Environ. Pollut. 159 (10), 2575–2585. https://doi.org/10.1016/j.envpol.2011.06.011.

Yan, N., Liu, W., Xie, H., Gao, L., Han, Y., Wang, M., Li, H., 2016. Distribution and assessment of heavy metals in the surface sediment of Yellow River China. J. Environ. Sci. 39 (1), 45–51. https://doi.org/10.1016/j.jes.2015.10.017.

Yan, Y., Wan, R.A., Yu, R.L., Hu, G.R., Lin, C.Q., Huang, H.B., 2022. A comprehensive analysis on source-specific ecological risk of metal (loid) s in surface sediments of mangrove wetlands in Jiulong River Estuary, China. Catena 209, 105817. https://doi.org/10.1016/j.catena.2021.105817.

Zhang, Q., Ying, G., Pan, C., Liu, Y., Zhao, J., 2015. Comprehensive evaluation of antibiotics emission and fate in the river basins of China: source analysis, multimedia modeling, and linkage to bacterial resistance. Environ. Sci. Technol. 49 https://doi.org/10.1021/acs.est.5b00729, 6772e6782.

Zhang, M., He, P., Qiao, G., Huang, J., Yuan, X., Li, Q., 2019. Heavy metal contamination assessment of surface sediments of the Subei Shoal, China: spatial distribution, source apportionment and ecological risk. Chemosphere 223, 211–222. https://doi.org/10.1016/j.chemosphere.2019.02.058.

Zhang, M., Wan, K., Zeng, J., Lin, W., Ye, C., Yu, X., 2020. Co-selection and stability of bacterial antibiotic resistance by arsenic pollution accidents in source water. Environ. Int. 135, 105351 https://doi.org/10.1016/j.envint.2019.105351.

Zhou, L., Meng, Y., Vaghefi, S., Marras, P., Sui, C., Lu, C., Abbaspour, K., 2020. Uncertainty-based metal budget assessment at the watershed scale: implications for environmental management practices. J. Hydrol. 584, 124699 https://doi.org/10.1016/j.jhydrol.2020.124699.

Zhang, J., Li, X., Guo, L., Deng, Z., Wang, D., Liu, L., 2021a. Assessment of heavy metal pollution and water quality characteristics of the reservoir control reaches in the middle Han River, China. Sci. Total Environ. 799, 149472 https://doi.org/10.1016/j.scitotenv.2021.149472.

Zhang, Y., Chen, J., Chen, H., Liu, L., Liu, C., Teng, Y., 2022a. An integrated multidisciplinary-based framework for characterizing environmental risks of heavy metals and their effects on antibiotic resistomes in agricultural soils. J. Hazard Mater. 426, 128113 https://doi.org/10.1016/j.jhazmat.2021.128113.

Zhang, Y., Liu, C., Chen, H., Chen, J., Li, J., Teng, Y., 2022b. Metagenomic insights into resistome coalescence in an urban sewage treatment plant-river system. Water Res. 224, 119061 https://doi.org/10.1016/j.watres.2022.119061.